

引用格式:臧贻萍,王钦贤,贾子策,等. 2026. 中国台湾地区古冷泉碳酸盐岩地质与地球化学特征[J]. 沉积学报, 44(2): 441-453.

ZANG YiPing, WANG QinXian, JIA ZiCe, et al. 2026. Geological and Geochemical Characteristics of Ancient Cold Seep Carbonates in Taiwan Area, China[J]. Acta Sedimentologica Sinica, 44(2): 441-453.

DOI: 10.14027/j.issn.1000-0550.2024.063

CSTR: 32268.14/j.cjxb.62-1038.2024.063

# 中国台湾地区古冷泉碳酸盐岩地质与地球化学特征

臧贻萍, 王钦贤, 贾子策, 陈多福

上海海洋大学海洋科学与生态环境学院, 上海 201306

**摘要** 【意义】冷泉活动对海洋生态系统及全球气候变化等具有重大影响,冷泉碳酸盐岩是海底冷泉活动形成的产物,其地质地球化学特征常被用于示踪渗漏流体信息及沉积环境变化。【进展】中国台湾地区冷泉碳酸盐岩主要发育于新生代中新世至更新世地层,是研究古冷泉的理想载体。对台湾地区冷泉碳酸盐岩发育的地质产状、矿物岩石学特征、碳氧同位素、稀土元素地球化学以及宏体生物化石等方面进行了系统阐述。【结论与展望】台湾地区冷泉碳酸盐岩以块状和烟囱状为主,分别指示了强度较弱的扩散和较强的喷溢流体活动;碳和氧同位素显示冷泉流体的碳源主要来自生物成因甲烷和热成因甲烷,并受海水或产甲烷残余CO<sub>2</sub>的影响;稀土元素地球化学特征显示冷泉碳酸盐岩形成于还原环境;冷泉生物以双壳类生物化石为主,中新世和上新世生物种类少,更新世生物种类多,可能受水深的控制。未来可从冷泉碳酸盐岩的微区原位碳和氧同位素分析、碳酸盐相矿物的Mo元素及其同位素分析,以及满月蛤科不同属生物化石发育的空间差异并结合地球化学分析等方面开展深入研究,以期完善对台湾地区古冷泉体系的理解。

**关键词** 碳酸盐岩;古冷泉;中国台湾地区;碳源;沉积环境;宏体生物

**第一作者** 臧贻萍,女,1997年出生,硕士研究生,海洋沉积,E-mail: zypde0907@126.com

**通信作者** 王钦贤,男,副研究员,E-mail: qxwang@shou.edu.cn

**中图分类号**:P736 **文献标志码**:A **文章编号**:1000-0550(2026)02-0441-13

## 0 引言

冷泉是指来自海底沉积界面之下,以碳氢化合物(天然气和石油)、硫化氢和水为主要成分,温度与海水相近的流体以扩散对流或渗漏喷溢的方式进入海底水体产生的一系列物理、化学及生物作用的现象(陈多福等,2002;Campbell,2006),其广泛发育在全球大陆边缘海底。在冷泉环境中渗漏的甲烷被厌氧氧化甲烷古菌(Anaerobic Methanotrophic Archaea, ANME)和硫酸盐还原细菌(Sulfate-Reducing Bacteria, SRB)共同介导的甲烷厌氧氧化反应( $\text{CH}_4 + \text{SO}_4^{2-} \rightarrow \text{HCO}_3^- + \text{HS}^- + \text{H}_2\text{O}$ , anaerobic oxidation of methane, AOM)所消耗(Boetius *et al.*, 2000),这一过程会使孔隙水的碱度增大,有利于碳酸盐类矿物的沉淀( $\text{Ca}^{2+} + 2\text{HCO}_3^- \rightarrow \text{CaCO}_3 + \text{CO}_2 + \text{H}_2\text{O}$ ),并形成冷泉碳酸盐岩(Feng and Chen, 2015; Feng *et al.*, 2018)。

因此,冷泉碳酸盐岩是冷泉活动的“指示剂”。

自Campbell和Bottjer在1993年提出寻找古冷泉研究计划以来,越来越多古冷泉活动的地质记录被发现(Kelly *et al.*, 1995; Peckmann *et al.*, 2002; Gill *et al.*, 2005; Hammer *et al.*, 2011; Smrzka *et al.*, 2017; Zwicker *et al.*, 2018)。迄今为止发现的古代冷泉碳酸盐岩发育时代主要集中在白垩纪和新生代,更早的古冷泉碳酸盐岩则较为少见,最古老的冷泉沉积可以追溯到约635 Ma 陡山沱组底部的“盖帽”碳酸盐岩(Jiang *et al.*, 2003)。古代冷泉碳酸盐岩主要有块状、丘状、结核状、烟囱状、细管状、壳层状等多种产状(Campbell, 2006; Chien *et al.*, 2012),不同形态碳酸盐岩可能与流体渗漏类型与强弱有关(Chien *et al.*, 2013)。冷泉碳酸盐岩的碳酸盐矿物主要包括高镁方解石(Mg>5%)、文石、低镁方解石和白云石等(Campbell *et al.*, 2002; Naehr *et al.*, 2007; Pierre *et al.*,

收稿日期:2024-04-15;修回日期:2024-05-02;录用日期:2024-06-03;网络出版日期:2024-06-03

基金项目:国家自然科学基金项目(42172110)

2016), 经历后期成岩作用的古代碳酸盐矿物主要为低镁方解石(Joseph *et al.*, 2013)。冷泉碳酸盐岩的碳同位素组成可以示踪渗漏流体的来源, 通常其 $\delta^{13}\text{C}$ 值低于 $-25\text{‰}$ (Campbell *et al.*, 2008), 但古代冷泉碳酸盐岩由于受到后期成岩作用、海水 $\text{SO}_4^{2-}$ 浓度和溶解无机碳(DIC)浓度变化等因素的影响, 其碳同位素值会发生一定程度的正偏(Campbell, 2006; Bristow and Grotzinger, 2013)。冷泉碳酸盐岩的稀土元素通常呈现出中稀土富集的“钟型”模式, Ce异常可以反映沉积环境的氧化还原条件(Jakubowicz *et al.*, 2015)。

台湾岛位于菲律宾海板块的吕宋岛弧与亚欧大陆边缘之间的碰撞带, 其中新世至更新世地层中广泛发育冷泉碳酸盐岩, 学者们对其矿物岩石学、碳和氧同位素等基础地质与地球化学特征开展进行了比较详细的研究(Huang *et al.*, 2006; Wang *et al.*, 2006; Chien *et al.*, 2012, 2013; Wang *et al.*, 2018; Blouet *et al.*, 2021; 赵若思等, 2021; Ge *et al.*, 2023)。本文系统总结了台湾地区冷泉碳酸盐岩的地质产状和矿物岩石学特征, 碳和氧同位素及稀土元素地球化学特征, 以及保存的宏体生物化石等特征, 并结合世界其他地区冷泉碳酸盐岩的地质和地球化学特征, 探讨了台湾地区冷泉碳酸盐岩所记录的流体渗漏活动和沉积环境特征, 进而提出了今后的研究重点。

## 1 地质背景

台湾岛位于亚洲大陆东南, 北连东海, 西为台湾海峡, 西南接南海, 南为吕宋海峡, 东临花东海盆和菲律宾海(Huang *et al.*, 2001)。台湾地区西南部及东北部海域分别存在着两个方向相反的马尼拉海沟及琉球海沟隐没带(Huang *et al.*, 2006)。双俯冲带显著控制了台湾岛及附近海域的地质特征与大地构造, 由西向东可分为海岸平原、西部麓山带、雪山山脉、中央山脉及海岸山脉五个地形构造单元。西部麓山带是典型的被动式大陆边缘沉积, 由晚渐新世、中新世至早更新世的浅海相沉积地层经推覆构造断层活动挤压变形而成, 是变形增生楔的前缘, 这种构造带促进了烃类流体的活动(Huang *et al.*, 2013; 黄博宏等, 2022)。因此, 在中新世至更新世地层中广泛发育烃类流体活动形成的冷泉碳酸盐岩, 是研究地质历史时期冷泉活动的天然实验室。

台湾地区冷泉碳酸盐岩主要发育于新生代的中新世至更新世的泥岩和页岩为主的地层中, 主要包

括台湾中部南投县国姓乡的中新世樟湖坑组泥页岩(Wang *et al.*, 2018)、台湾南部高雄市甲仙地区(白云仙谷、牛埔、四德巷)的新世盐水坑组页岩(Guan *et al.*, 2019; Blouet *et al.*, 2021), 以及台湾西南部高雄市大岗山、小岗山、半屏山和寿山地区的更新世古亭坑组泥岩(Wang *et al.*, 2006)。此外, 在凤山地区的更新世大社组泥岩中也有少量冷泉碳酸盐岩露头发育(王士伟, 2006)(图1)。

## 2 地质产状

台湾岛不同地区发育的冷泉碳酸盐岩在野外的产状主要有两类(表1): 一类是几十厘米到几米大小的结核状、透镜状和块状等个体较大的冷泉碳酸盐岩(图2a, b, g), 主要发育在四德巷、白云仙谷、凤山、寿山和半屏山地区, 以及大岗山和小岗山地区(表1)。第二种产出类型为巨型烟囱状或管状冷泉碳酸盐岩(图2c~f), 甲仙地区四德巷剖面 and 国姓乡主要为此类冷泉碳酸盐岩(表1)。甲仙地区牛埔剖面冷泉碳酸盐岩以细管状网络为主(图2d), 大岗山和小岗山地区也发育少许管状冷泉碳酸盐岩。此外, 在国姓乡, 管状碳酸盐岩通常与烟囱状碳酸盐岩伴生(图2f), 而在大岗山和小岗山地区, 管状碳酸盐岩通常与块状碳酸盐岩伴生(图2g)。

冷泉碳酸盐岩是甲烷在硫酸盐—甲烷转换带(Sulfate Methane Transition Zone, SMTZ)经甲烷厌氧氧化古菌作用形成的产物, 它代表了古代冷泉流体活动的区域, 其产状可以反映流体活动的类型及强弱(Chien *et al.*, 2013)。四德巷、白云仙谷和三山地区(凤山、寿山、半屏山)以及大岗山和小岗山地区均发育块状层或个体较大的结核状冷泉碳酸盐岩, Wang *et al.* (2006)和Chien *et al.* (2013)认为这是由渗漏强度较弱但流量较大的流体以扩散运移方式形成, 可能经历了较长时间的冷泉活动, 其产状与发育于地中海盆地的中新世角砾化块状冷泉碳酸盐岩相似(Iadanza *et al.*, 2013)。Bahr *et al.* (2010)和Iadanza *et al.* (2013)研究发现碳酸盐岩的原位角砾化现象与烃类物质运移和流体超压有关。管状和烟囱状冷泉碳酸盐岩在冷泉系统中较为常见, 四德巷和国姓乡的管状和烟囱状冷泉碳酸盐岩与加利福尼亚蒙特利湾现代冷泉碳酸盐岩产状类似(Stakes *et al.*, 1999), Stakes *et al.* (1999)认为这可能是渗漏通量较高的甲烷流体在比较集中的通道状态下形成的产物, 相对于

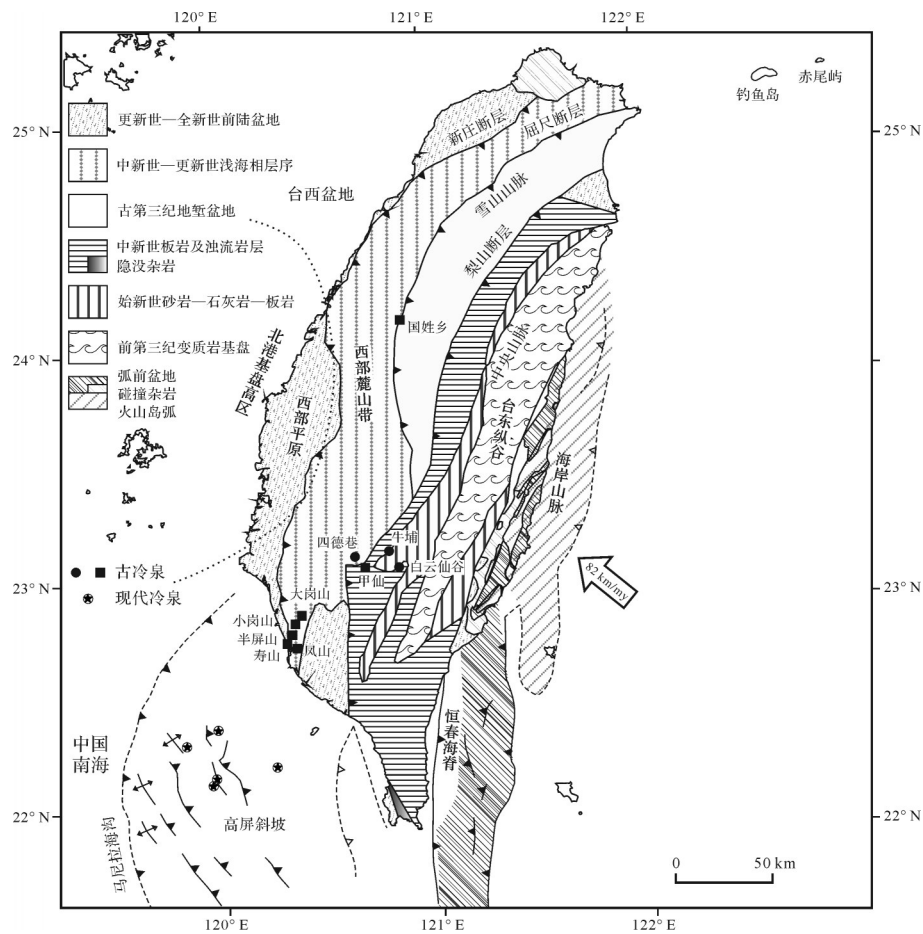


图1 中国台湾地区地质构造及冷泉碳酸盐岩发育位置(据 Huang *et al.*, 2000, 2012 修改)

图中黑色方形代表古冷泉发育的地区,黑色圆形代表剖面发育的位置

Fig.1 Geological structure and development location of cold seep carbonates in Taiwan area, China (modified from Huang *et al.*, 2000, 2012)

Black squares represent the areas where ancient cold seeps developed; Black circles represent the locations of developed sections

个体较大的块状或结核状冷泉碳酸盐岩其受冷泉活动影响的时间可能较短。管状冷泉碳酸盐岩可以连接形成网络状,如甲仙地区牛埔剖面广泛发育网络细管状冷泉碳酸盐岩。Chien *et al.* (2013)认为该类网络管状结构可能是由渗漏强度较强的流体沿着层面或岩体裂隙的较小通道所形成。此外,世界其他地区也存在不同产状冷泉碳酸盐岩共生的现象(Nyman and Nelson, 2011; Iadanza *et al.*, 2013; Reitner *et al.*, 2015; Zhang *et al.*, 2016),如 Nyman and Nelson (2011)在新西兰 Taranaki 盆地中新世地层中发现结核状或块状与管状或烟囱状冷泉碳酸盐岩共生,推测管状或烟囱状碳酸盐岩形成于冷泉活动早期较高的  $\text{Ca}^{2+}$  浓度、 $\text{SO}_4^{2-}$  浓度和压强环境,结核状或块状碳酸盐岩则形成于晚期相对较低的  $\text{Ca}^{2+}$  浓度、 $\text{SO}_4^{2-}$  浓度和压强环境。但与新西兰地区共生碳酸盐岩几乎发育于同一层位

不同,台湾四德巷剖面烟囱状冷泉碳酸盐岩出露的层位普遍高于结核状碳酸盐岩(Chien *et al.*, 2013),这可能与地质构造运动导致的渗漏流体强度变化有关(Nyman and Nelson, 2011; Chien *et al.*, 2013)。

### 3 矿物学与岩石学

冷泉碳酸盐岩的矿物岩石学特征可以示踪流体来源,反映其沉淀环境。台湾地区冷泉碳酸盐岩的岩石薄片观察显示国姓乡和甲仙地区(四德巷、牛埔、白云仙谷)碳酸盐矿物大多以泥晶或微晶的形式产出,且广泛发育草莓状黄铁矿(图3)(Wang *et al.*, 2018; 赵若思等, 2021)。两地均含有石英和长石陆源碎屑(图3a, b)以及生物碎屑,并保存较完好的有孔虫化石(图3d)(Wang *et al.*, 2018; Blouet *et al.*, 2021)。矿物组成分析显示碳酸盐相矿物以方解石

表1 台湾地区冷泉碳酸盐岩野外产状、主要碳酸盐矿物特征

Table 1 Field occurrences and main carbonate minerals in cold seep carbonates, Taiwan area

地区	冷泉碳酸盐岩形态与构造	主要矿物及含量	文献
	大型角砾状结核有些具有喷口与管状构造		
甲仙四德巷	巨型烟囱含气孔与管路状构造 细管状网络	白云石:25%~83%;方解石:2%~51%	Chien <i>et al.</i> , 2013; Blouet <i>et al.</i> , 2021; 赵若思等, 2021;
甲仙牛埔	细管状网络	白云石:33%~67%;方解石:8%~24%	Ge <i>et al.</i> , 2023
甲仙白云仙谷	透镜状	白云石:52%~88%;方解石:0%~10%	
国姓乡	管状和烟囱状	白云石:7%~83%;方解石:0%~60%	Wang <i>et al.</i> , 2018
大岗山水泥矿场	块状和管状	白云石:7%~81%;方解石:5%~75%	
小岗山	块状、结核状、管状		
凤山石灰岩矿场	块状	白云石:67%;方解石:6%	王士伟, 2006;
寿山采石场	结核状		Wang <i>et al.</i> , 2006
半屏山石灰岩采矿场	块状	白云石:10%~62%;方解石:7%~72%	

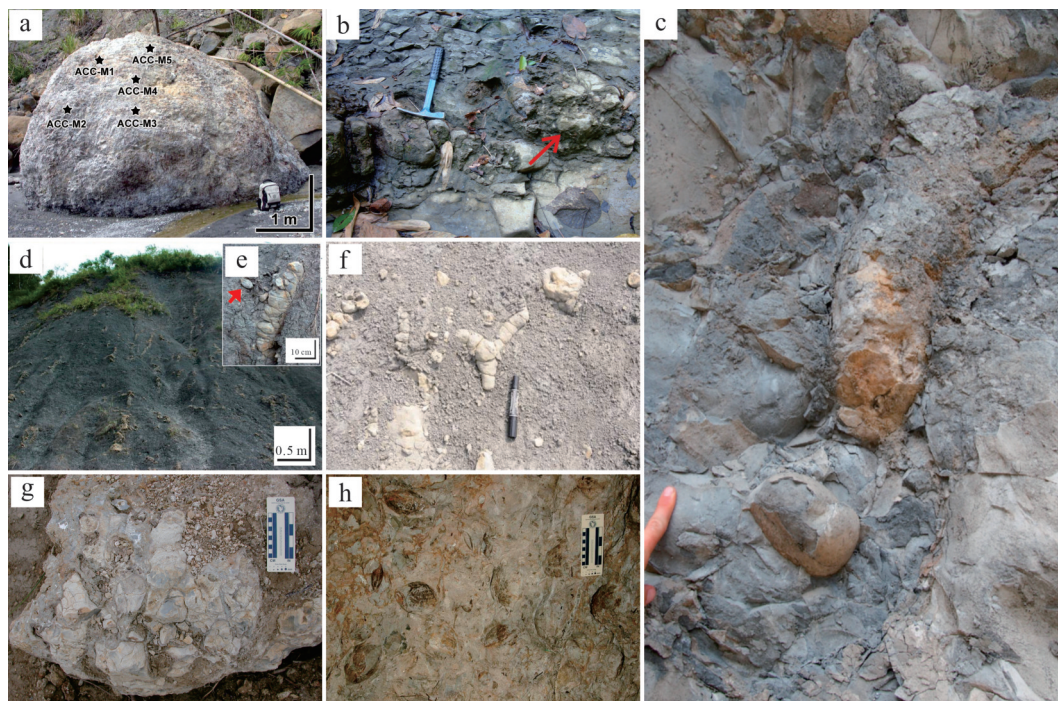


图2 台湾地区冷泉碳酸盐岩野外产状特征

(a) 甲仙地区四德巷剖面大型结核状冷泉碳酸盐岩 (Chien *et al.*, 2013); (b) 甲仙地区白云仙谷剖面透镜状冷泉碳酸盐岩 (赵若思等, 2021); (c) 四德巷剖面显示巨型烟囱状冷泉碳酸盐岩及其下部凸出的满月蛤类 *Anodontia goliath* 化石 (Blouet *et al.*, 2021); (d) 甲仙地区牛埔剖面浅色细管状冷泉碳酸盐岩发育于深灰色的泥质碎屑岩中 (Chien *et al.*, 2013); (e) 为 (d) 中的管状局部特写且箭头指示满月蛤类 *Lucinoma annulata* (Reeve) 化石 (Chien *et al.*, 2013); (f) 国姓乡管状冷泉碳酸盐岩 (Wang *et al.*, 2018); (g) 小岗山地区块状冷泉碳酸盐岩, 其内有许多碳酸盐胶结的管状构造 (王士伟, 2006); (h) 大岗山地区块状冷泉碳酸盐岩中富含巨带蛤化石 (王士伟, 2006)

Fig.2 Photographs of cold seep carbonate outcrops in Taiwan area

(a) large nodules in Sidexiang section, Chiahhsien (Chien *et al.*, 2013); (b) lenticular outcrops in Baiyunxiangu section, Chiahhsien (Zhao *et al.*, 2021); (c) giant chimney outcrop in Sidexiang section, showing bulbous fossil of *Anodontia goliath* (Blouet *et al.*, 2021); (d) light-colored tubular outcrops in dark gray argillaceous clastic rocks, Niupu section (Chien *et al.*, 2013); (e) photo enlargement of tubular carbonate in (d); *Lucinoma annulata* (Reeve) fossil indicated by arrow (Chien *et al.*, 2013); (f) tubular outcrops, Guoxing township area (Wang *et al.*, 2018); (g) blocky outcrop with many carbonate cemented tubular structures, Hsiaokangshan area (Wang, 2006); (h) *Lucinoma*-enriched outcrop, Takangshan area (Wang, 2006)

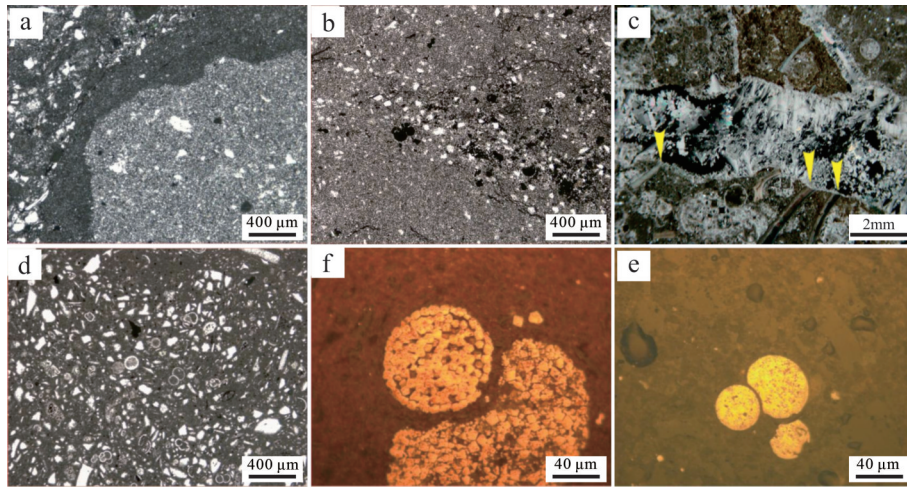


图3 台湾地区冷泉碳酸盐岩岩石学显微特征

(a)甲仙地区冷泉碳酸盐岩基质呈现两种不同成分,黑色泥晶和灰色微晶,含少量陆源碎屑,单偏光(Wang *et al.*, 2018);(b)国姓乡泥微晶碳酸盐岩,黑色圆形部分为草莓状黄铁矿,发育不规则丝状体,单偏光(Wang *et al.*, 2018);(c)大岗山地区碳酸盐脉状裂隙充填岩样,箭头指示贝类壳体在脉状充填处断裂,单偏光(王士伟, 2006);(d)国姓乡生物碎屑泥晶碳酸盐岩,含大量保存完整的有孔虫化石,单偏光(Wang *et al.*, 2018);(e)国姓乡草莓状黄铁矿集合体,反射光(Wang *et al.*, 2018);(f)甲仙地区草莓状黄铁矿充填在有孔虫房室内,反射光(Wang *et al.*, 2018)

Fig.3 Microscopic petrologies of cold seep carbonates in Taiwan area

(a) cold seep carbonate matrix, Chiahsien area, with black micrite and gray microcrystals and a small amount of terrigenous debris, plane polarized light (PPL) (Wang *et al.*, 2018); (b) mud microcrystalline carbonates, Guoxing township area, showing strawberry pyrites (black circles) and development of irregular filaments, PPL (Wang *et al.*, 2018); (c) fracture with carbonate vein infill, Takangshan area, with arrows showing broken shellfish shells at the vein, PPL (Wang, 2006); (d) bioclastic micritic carbonates, Guoxing township area, containing multiple intact Foraminifera fossils, PPL (Wang *et al.*, 2018); (e) strawberry pyrite aggregate, Guoxing township area, reflected light (RL) (Wang *et al.*, 2018); (f) strawberry pyrites filling Foraminifera spaces, Chiahsien area, RL (Wang *et al.*, 2018)

和白云石为主,不含文石(表1)。甲仙地区(四德巷、牛埔、白云仙谷)和半屏山、凤山地区冷泉碳酸盐岩以白云石为主,不含或含少量方解石,国姓乡与大岗山地区以白云石和方解石为主。其中,白云仙谷地区冷泉碳酸盐岩中白云石含量普遍较高,最高可达88%(表1)(赵若思等, 2021)。

已有的研究发现,包括台湾地区在内的众多古代冷泉碳酸盐岩均不含文石(Birgel *et al.*, 2006; Viola *et al.*, 2015; Lu *et al.*, 2023),可能由于文石属于亚稳态矿物,在成岩作用下极容易转变为方解石,若受白云石化作用影响亦可转变为白云石,因此古代冷泉碳酸盐岩其白云石与方解石含量通常较高,不含文石(Chien *et al.*, 2013)。原生白云岩的成因问题一直是研究的热点,现代海底冷泉碳酸盐岩中广泛发育白云石,可能是解开该问题的钥匙。Takeuchi *et al.* (2007)通过对日本黑岛烟囱状白云岩的研究认为冷泉环境有利于原生白云石的沉淀。Bian *et al.* (2013)对墨西哥湾GC140站位冷泉白云岩进行扫描电镜分析,观察到原生白云石特有的多结节纹理结构(knobly texture),证明白云岩为原生沉淀。Tong *et al.* (2019)对墨西哥湾北部GC140和GB382站位冷泉碳酸盐岩白云石中碳酸盐晶格硫(CAS)的 $\delta^{18}O/\delta^{34}S$

斜率和铬还原性硫(CRS)的 $\delta^{34}S_{CRS}$ 进行分析,发现二者均高于高镁方解石和文石,据此推测白云石的沉淀位置可能位于较深处的SMTZ带及以下区域(产甲烷带),沉积环境可能为硫酸盐浓度较低但硫化物浓度较高的还原环境。

台湾地区冷泉碳酸盐岩中白云石含量较高,赵若思等(2021)认为其可能为受微生物硫酸盐还原作用促进而形成的原生白云石。Chien *et al.* (2013)发现台湾地区冷泉碳酸盐岩具有复杂的白云石含量模式,推测它们可能是受原生与次生作用的综合影响,并很可能由次生作用主导。此外,国姓乡草莓状黄铁矿附近发育的不规则丝状体(图3b)与黑海地区现代冷泉碳酸盐岩中发育的丝状体类似,被认为是石化的甲烷厌氧氧化古菌(Peckmann *et al.*, 2001),可能与AOM反应中的生物化学过程有关(Wang *et al.*, 2018)。目前对台湾地区白云石的成因还未达成共识,后续可以结合扫描电镜分析白云石微观结构以及白云石的硫氧同位素特征进一步探讨。

草莓状黄铁矿的出现通常与甲烷厌氧氧化作用有关,且其粒径大小可以指示沉积时的氧化还原环境(Wilkin *et al.*, 1996; 崔娜等, 2023)。Wilkin *et al.* (1996)和Rickard(2019)认为氧化或弱氧化环境中形

成的草莓状黄铁矿粒径普遍较大,还原或硫化环境中形成的草莓状黄铁矿粒径通常较小(Wilkin *et al.*, 1996; Rickard, 2019; 崔娜等, 2023)。有研究对台湾地区国姓和甲仙地区的草莓状黄铁矿粒径进行了粗略判断,推测国姓乡较大的草莓状黄铁矿粒径指示其可能形成于氧化环境,而甲仙地区草莓状黄铁矿粒径较小,指示其可能形成于还原环境(王钦贤, 2014)。而林杞(2016)研究发现,形成于SMTZ带内的草莓状黄铁矿的粒径特征无法有效反映沉积环境的氧化还原条件,且较大粒径的草莓状黄铁矿可能指示了较强的AOM作用和SMTZ带的位置。Miao *et al.* (2021)将形成于SMTZ带内的草莓状黄铁矿与形成于正常海相沉积环境中的黄铁矿粒径大小进行对比,也发现SMTZ带内草莓状黄铁矿粒径明显偏大的现象。因此,国姓乡较大的草莓状黄铁矿粒径可能指示其形成于更强的还原性冷泉渗漏环境,并非氧化环境。但目前还未有针对台湾地区草莓状黄铁矿粒径大小的详细统计,未来有待开展该方面工作以探讨草莓状黄铁矿粒径大小与沉积环境氧化还原性的联系。

## 4 成岩流体及沉积环境判别方法

### 4.1 碳和氧同位素

冷泉碳酸盐岩的碳同位素主要继承了流体中烃类化合物(甲烷及重烃)的碳同位素特征,可以指示流体来源(Peckmann *et al.*, 2002; Campbell *et al.*, 2008)。冷泉流体的碳源可能有:(1)生物成因甲烷( $\delta^{13}\text{C} < -50\text{‰}$ );(2)热成因甲烷( $\delta^{13}\text{C} = -50\text{‰} \sim -30\text{‰}$ );(3)石油烃类物质( $\delta^{13}\text{C} = -35\text{‰} \sim -25\text{‰}$ );(4)海水

( $\delta^{13}\text{C} = 0 \sim \pm 3\text{‰}$ );(5)产甲烷过程中残余的 $\text{CO}_2$ ( $\delta^{13}\text{C} > +5\text{‰}$ )(Campbell, 2006)。台湾地区冷泉碳酸盐岩的 $\delta^{13}\text{C}$ 值介于 $-53.7\text{‰} \sim +9.0\text{‰}$ (图4, 5)。其中,中新世 $\delta^{13}\text{C}$ 值介于 $-51.8\text{‰} \sim -20.9\text{‰}$ (Chien *et al.*, 2012; Wang *et al.*, 2018),上新世 $\delta^{13}\text{C}$ 值介于 $-49.6\text{‰} \sim +9.0\text{‰}$ (Wang *et al.*, 2006; Chien *et al.*, 2013; Guan *et al.*, 2019; Blouet *et al.*, 2021; Ge *et al.*, 2023),更新世 $\delta^{13}\text{C}$ 值介于 $-53.7\text{‰} \sim -4.3\text{‰}$ (Wang *et al.*, 2006)。Wang *et al.* (2018)研究显示中新世冷泉碳酸盐岩碳同位素受到成岩作用改造,进而利用其最小端元值接近 $-50\text{‰}$ ,推测碳源主要来自生物成因甲烷。Guan *et al.* (2019)认为上新世冷泉碳酸盐岩的碳源包括生物成因甲烷(四德巷地区)、热成因甲烷或原油等重烃(白云仙谷地区)以及产甲烷残余 $\text{CO}_2$ (牛埔地区),而Blouet *et al.* (2021)和Ge *et al.* (2023)认为上新世冷泉碳酸盐岩还受海水来源碳的影响。对于更新世冷泉流体的碳源,Wang *et al.* (2006)认为可能来自生物成因甲烷和热成因甲烷。总体上,台湾地区冷泉碳酸盐岩碳源以生物成因和热成因甲烷为主,并受碳同位素值偏正的流体(海水或产甲烷残余 $\text{CO}_2$ )影响,上新世冷泉流体的碳源类型最为复杂。Chen *et al.* (2017)对台西南海域现代活动冷泉的研究发现,冷泉流体类型变化与构造活动有关,如生物成因甲烷多形成于被动大陆边缘,而热成因甲烷则多被发现于主动大陆边缘尤其是斜坡和陆上泥火山的沉积物中。上新世台湾地区正处于台湾造山带形成时期的弧—陆碰撞阶段(黄博宏等, 2022),冷泉碳酸盐岩集中发育的甲仙地区形成了广泛的逆冲断层、隐没断层以及向斜、背斜的褶皱带(Ge *et al.*, 2023),因此上

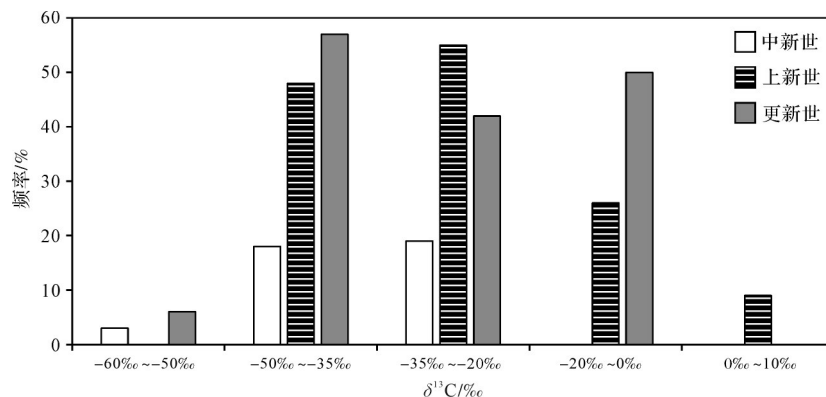


图4 台湾地区冷泉碳酸盐岩碳同位素分布(数据来源于Huang *et al.*, 2006; Wang *et al.*, 2006; Chien *et al.*, 2012, 2013; Wang *et al.*, 2018; Guan *et al.*, 2019; 赵若思等, 2021; Ge *et al.*, 2023)

Fig.4 Carbon isotope distribution in cold seep carbonates, Taiwan area (data from Huang *et al.*, 2006; Wang *et al.*, 2006; Chien *et al.*, 2012, 2013; Wang *et al.*, 2018; Guan *et al.*, 2019; Zhao *et al.*, 2021; Ge *et al.*, 2023)

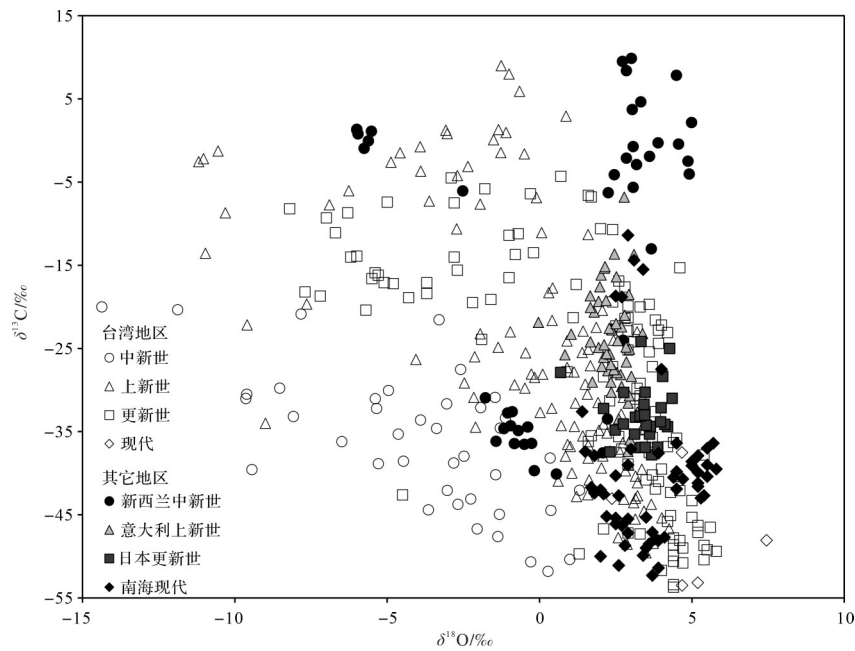


图5 台湾地区及其他地区冷泉碳酸盐岩碳氧同位素组成(数据来源于 Huang *et al.*, 2006; Wang *et al.*, 2006; Nyman and Nelson, 2011; Chien *et al.*, 2012, 2013; Tong *et al.*, 2013; Utsunomiya *et al.*, 2015; Liang *et al.*, 2017; Wang *et al.*, 2018; Guan *et al.*, 2019; 赵若思等, 2021; Ge *et al.*, 2023; Perri *et al.*, 2024)

Fig.5 Carbon and oxygen isotope compositions in cold seep carbonates in Taiwan and other areas (data from Huang *et al.*, 2006; Wang *et al.*, 2006; Nyman and Nelson, 2011; Chien *et al.*, 2012, 2013; Tong *et al.*, 2013; Utsunomiya *et al.*, 2015; Liang *et al.*, 2017; Wang *et al.*, 2018; Guan *et al.*, 2019; Zhao *et al.*, 2021; Ge *et al.*, 2023; Perri *et al.*, 2024)

新世冷泉流体碳源类型的多样性可能与该地区复杂的地质构造有关。

冷泉碳酸盐岩的氧同位素可以作为评估其受成岩作用影响程度的指标,亦可以反映形成时的温度,并指示冷泉流体的氧同位素组成(Arthur *et al.*, 1983; Shields and Stille, 2001; Campbell, 2006)。台湾地区冷泉碳酸盐岩 $\delta^{18}\text{O}$ 值介于 $-14.4\text{‰}\sim+5.8\text{‰}$ (图5)。其中,中新世 $\delta^{18}\text{O}$ 值介于 $-14.4\text{‰}\sim+1.3\text{‰}$ (Chien *et al.*, 2012; Wang *et al.*, 2018),上新世 $\delta^{18}\text{O}$ 值介于 $-11.2\text{‰}\sim+4.3\text{‰}$ (Wang *et al.*, 2006; Chien *et al.*, 2013; Guan *et al.*, 2019; Blouet *et al.*, 2021; Ge *et al.*, 2023),更新世 $\delta^{18}\text{O}$ 值介于 $-8.2\text{‰}\sim+5.8\text{‰}$ (Wang *et al.*, 2006)。Chien *et al.*(2012)根据海底水温与氧同位素分馏方程计算出台湾地区中新世冷泉碳酸盐岩的沉积温度高达 $84\text{ }^{\circ}\text{C}$ ,明显超过了现代海底冷泉流体的温度,推测氧同位素可能受到 $\delta^{18}\text{O}$ 亏损的地下水或者低镁方解石脉的影响,但并未考虑氧同位素可能已受到后期成岩作用的改造,从而无法反映沉积温度与初始流体信息。Wang *et al.*(2006)和Wang *et al.*(2018)根据 $\delta^{18}\text{O}$ 值判断台湾地区中新世和上新世冷泉碳酸盐岩均受到较强的后期成岩改造,而更新世受成岩改造程度较弱,并且利用中新世冷泉碳酸盐

岩 $\delta^{18}\text{O}$ 端元值计算出该时期冷泉流体的温度约为 $20\text{ }^{\circ}\text{C}$ 。此外,Wang *et al.*(2006)根据更新世不同矿物组成的冷泉碳酸盐岩 $\delta^{18}\text{O}$ 值存在较大差异,进一步推测两种碳酸盐矿物(方解石、白云石)形成于不同时期。这与新西兰中新世Taranaki盆地方解石质和白云石质碳酸盐岩的 $\delta^{18}\text{O}$ 值差异较大类似(图5)。Nyman and Nelson(2011)认为 $\delta^{18}\text{O}$ 值偏负的方解石质碳酸盐岩形成于天然气水合物形成时期,而 $\delta^{18}\text{O}$ 值偏正的白云石质碳酸盐岩形成于天然气水合物分解释放时期。台湾地区从中新世到更新世的冷泉碳酸盐岩 $\delta^{18}\text{O}$ 值呈现逐渐变正的趋势(图5),可能指示其经历了从天然气水合物形成到分解释放的过程。此外,与世界其他地区同时期冷泉碳酸盐岩 $\delta^{18}\text{O}$ 值相比较,中新世和上新世以及部分更新世冷泉碳酸盐岩的 $\delta^{18}\text{O}$ 值均偏负(图5),可能说明台湾地区总体上受成岩作用(如大气降水(Ge *et al.*, 2023))影响程度较大。

以上的研究大多是利用冷泉碳酸盐岩的全岩碳氧同位素来分析冷泉流体来源。Ge *et al.*(2023)发现台湾甲仙地区部分点位冷泉碳酸盐岩明显形成于多期次流体,同一样品不同微区的碳氧同位素存在显著的差异,而全岩碳氧同位素则无法区分不同期次

流体。因此,未来可以开展微区碳氧同位素分析,更精确地还原地质历史时期的流体活动特征。

#### 4.2 稀土元素及其他

稀土元素地球化学特征可以提供沉积环境和沉积流体的相关信息。后太古宙澳大利亚页岩(Post-Archean Australian Shale, PAAS)标准化稀土元素配分模式可以区分不同的沉积环境,Ce异常可以指示沉积环境的氧化还原特征(赵彦彦等,2019)。台湾国姓和甲仙地区中新世和上新世冷泉碳酸盐岩稀土元素配分模式呈现中稀土富集的“钟型”模式,无Ce异常或轻微Ce正异常(图6),指示还原的沉积特征(Wang *et al.*, 2018; Ge *et al.*, 2023)。更新世冷泉碳酸盐岩稀土元素未见报道。除台湾地区冷泉碳酸盐岩外,其他地区(如墨西哥湾、西藏)冷泉环境中自生碳酸盐岩的稀土元素配分模式也多表现出中稀土富集的“钟型”模式特征(Hu *et al.*, 2014; 张文进等, 2018)。Tribovillard *et al.* (2013)认为这种中稀土富集的特征可能与冷泉碳酸盐岩富集铁锰等元素有关。Birgel *et al.* (2011)发现墨西哥湾现代冷泉碳酸盐岩沉积环境具有动态的变化特征,可能与流体渗漏通量的变化有关。目前对台湾地区稀土元素的研究仅集中在国姓和甲仙地区,其他区域还未有稀土元素研究的报道,未来有待进一步丰富台湾地区冷泉碳酸盐岩的稀土元素数据库。

除还原性沉积环境外,冷泉碳酸盐岩也可能沉淀于海底深部较封闭的硫化环境,而稀土元素虽然可以有效区分沉积环境的氧化还原特征,却无法示

踪硫化环境。近年来,Mo的元素丰度和同位素组成特征被用于识别硫化环境(Hutchings *et al.*, 2020; Ye *et al.*, 2021),如形成于硫化环境中的沉积物通常具有较高的Mo浓度(>60  $\mu\text{g/g}$ )(Scott and Lyons, 2012)且Re/Mo比值接近海水值,而缺氧非硫化环境中沉积物的Re/Mo比值高于海水值(Crusius and Thomson, 2000; Scholz *et al.*, 2013)。此外,前文已提及利用黄铁矿粒径大小可以示踪沉积环境的氧化还原特征。未来或许可以结合这两种方法来判断台湾地区冷泉碳酸盐岩是否形成于硫化环境。

## 5 冷泉碳酸盐岩宏体生物化石

冷泉碳酸盐岩中发育的生物化石群落是辨认古冷泉的重要依据,这些海底冷泉生物与硫化物氧化菌和/或甲烷氧化菌共生,通过硫化物和/或甲烷氧化反应来获得维持生命代谢活动所需的能量(Dubilier *et al.*, 2008),是探索地球极端环境生命生存与演化的重要窗口。台湾地区冷泉碳酸盐岩发育了丰富的宏体生物化石(表2、图2c, e, h),以双壳贝类丰度最大(Kiel *et al.*, 2024)。其中,中新世和上新世宏体生物化石以满月蛤科的 *Meganodontia* 和 *Lucinoma* 为主(Chien *et al.*, 2012; Blouet *et al.*, 2021; Kiel *et al.*, 2024),更新世宏体生物化石主要包括满月蛤科的 *Meganodontia* 和 *Lucinoma*、贻贝科的 *Gigantidas*、雪爪蛤科的 *Isorropodon* 和未确定所属科的 *Sisonia* (Wang *et al.*, 2006; Kiel *et al.*, 2024)。

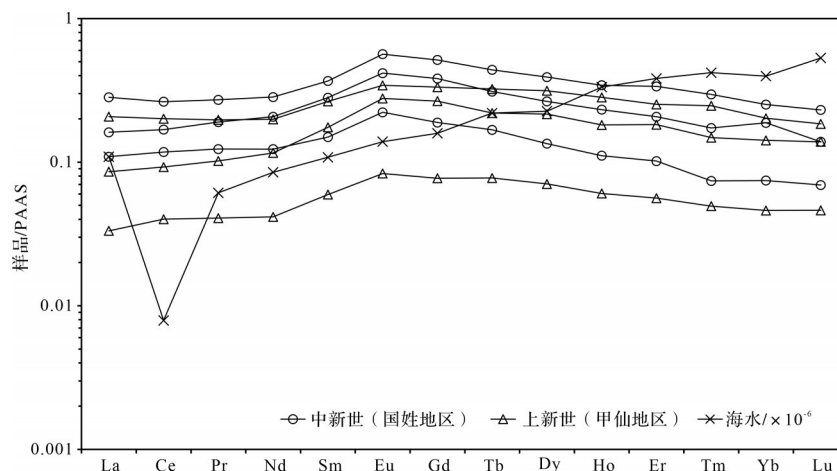


图6 台湾地区冷泉碳酸盐岩及现代海水稀土元素配分模式

(数据来源于 Freslon *et al.*, 2014; Wang *et al.*, 2018; 赵若思等, 2021; Ge *et al.*, 2023)

Fig.6 Distributions of rare earth element (REE) in modern seawater and cold seep carbonates, Taiwan area

(data from Freslon *et al.*, 2014; Wang *et al.*, 2018; Zhao *et al.*, 2021; Ge *et al.*, 2023)

表2 台湾地区冷泉碳酸盐岩宏体生物分类(据 Kiel *et al.*, 2024修改)  
Table 2 Macrofossil classifications in cold seep carbonates, Taiwan area  
(modified from Kiel *et al.*, 2024)

科	属			
	中新世	上新世	更新世	现代
<i>Bathymodiolinae</i>			<i>Gigantidas</i>	<i>Gigantidas</i> <i>Bathymodiolus</i>
<i>Thyasiridae</i>				<i>Conchocele</i> <i>Channelaxinus</i>
<i>Lucinidae</i>	<i>Meganodontia</i> <i>Lucinoma</i>	<i>Meganodontia</i> <i>Lucinoma</i>	<i>Meganodontia</i> <i>Lucinoma</i>	<i>Meganodontia</i> <i>Lucinoma</i>
<i>Vesicomiyida</i>			<i>Isorropodon</i>	<i>Isorropodon</i> <i>Archivesica</i>
未确认			<i>Sisonia</i>	

台湾地区中新世和上新世冷泉碳酸盐岩宏体生物以两种营内表栖(infaunal)生活的大型双壳类生物满月蛤科为主,明显少于同时期世界其他地区冷泉碳酸盐岩宏体生物化石的种类(Kiel and Hansen, 2015; Kiel *et al.*, 2020; Amano *et al.*, 2022)。考虑到满月蛤科生物通常生活于沉积物最顶部数十厘米深处且紧邻氧化还原界面(Stanley, 1970; Taylor and Glover, 2000), Kiel *et al.* (2024)认为宏体生物化石的种类可能是受到了水深的影响。相比之下,上新世冷泉碳酸盐岩中宏体生物化石种类更多,除满月蛤科外,还包括营外表栖(epifaunal)或半内表栖(semi-faunal)生活的 *Gigantidas horikoshii* 和 *Sisonia* 等生物(Kiel *et al.*, 2024)。现存的 *Gigantidas horikoshii* 生物被发现生活在水深 500 m 左右(Mellado *et al.*, 2022), Kiel *et al.* (2024)由此推测更新世冷泉碳酸盐岩形成于水深较深处,而中新世和上新世冷泉碳酸盐岩形成于水深较浅处。此外,简至炜(2014)发现冷泉碳酸盐岩宏体生物化石的体型尺寸可能与碳酸盐岩块体的大小有关,在甲仙地区发育的满月蛤科化石中,体型大的 *Meganodontia goliath* 往往伴随大型的自生性碳酸盐岩丘(如大型角砾状结核、巨型烟囱),而体型小的 *Lucinoma annulata* 则主要发育在较小型的自生性碳酸盐岩丘(如细管状网络)中,但对该现象产生的原因并未进行探讨。有关现代南海活动冷泉双壳类生物的研究发现,部分利用硫化氢的个体体型要大于利用甲烷的个体体型(Wang *et al.*, 2022),并且利用甲烷的贻贝表现出 La 异常和 LREE 富集(Wang *et al.*, 2020)。因此,冷泉生物的体型大小可能与其体内共生菌类型有关,未来可针对台湾地区满月蛤科不同属生物化石的稀土元素地球化学特征和发育差异开展进一步研究,以探讨其记录的冷泉流体信息以及与水深的联系。

## 6 结论与展望

台湾地区沿西部麓山带中新世至更新世地层中发育块状或烟囱状为主的冷泉碳酸盐岩,碳酸盐矿物组成以白云石和方解石为主,并广泛发育草莓状黄铁矿。冷泉碳酸盐岩碳同位素显示碳源主要来自生物成因甲烷和热成因甲烷,并受海水或产甲烷残余 CO<sub>2</sub> 影响。稀土元素配分模式指示冷泉碳酸盐岩沉积于还原环境。冷泉碳酸盐岩宏体生物化石以双壳类为主,中新世和上新世丰度较低,更新世丰度较高,可能受水深影响。

台湾地区冷泉碳酸盐岩可能发育多期次的流体活动,未来的研究方向可以考虑:开展原位微区碳氧同位素分析,以精确判断由多期次流体形成的冷泉碳酸盐岩的碳源;开展碳酸盐矿物相的主微量元素分析,重点利用 Mo 元素和同位素特征识别冷泉中的硫化环境;对满月蛤科不同属的宏体生物化石开展地球化学分析,探讨其记录的冷泉流体信息及与水深的联系。此外,台湾地区冷泉碳酸盐岩中白云石与方解石共生,针对白云石成因开展微区研究,有助于解开原生白云石成因之谜。

## 参考文献(References)

- 陈多福,陈先沛,陈光谦. 2002. 冷泉流体沉积碳酸盐岩的地质地球化学特征[J]. 沉积学报, 20(1): 34-40. [Chen Duofu, Chen Xianpei, Chen Guangqian. 2002. Geology and geochemistry of cold seepage and venting-related carbonates[J]. Acta Sedimentologica Sinica, 20(1): 34-40.]
- 崔娜,王钦贤,贾子策,等. 2023. 台湾国姓地区中新世海相菱铁矿结核成因:来自草莓状黄铁矿粒径和硫同位素的证据[原文如此][J]. 矿物岩石地球化学通报, 42(6): 1372-1379. [Cui Na, Wang Qinxian, Jia Zice, et al. 2023. Genesis of siderite nodules in Miocene marine sediment in the Kuohsing area, Taiwan, China: Evidences from particle sizes and sulfur isotopes of pyrite framboids[sic][J]. Bulletin of Mineralogy, Petrology and Geochemistry, 42(6): 1372-1379.]

- 黄博宏,魏春景,季建清. 2022. 再论台湾造山带构造格架与演化过程[J]. 岩石学报, 38(4): 963-979. [Huang Bohong, Wei Chunjing, Ji Jianqing. 2022. Tectonic framework and evolution of the Taiwan orogen: A revisit[J]. *Acta Petrologica Sinica*, 38(4): 963-979.]
- 简至炜. 2014. 台湾西南部西部麓山带甲仙地区上新世古冷泉自生性碳酸盐及其有孔虫群集之研究[D]. 台南:台湾成功大学: 12-79. [Chien Chih-Wei. 2014. Study of authigenic carbonates and associated foraminiferal assemblages in the Pliocene paleoseeps of Chiahhsien area in western Foothills, southwestern Taiwan[D]. Tainan, China: Taiwan Cheng Kung University: 12-79.]
- 林杞. 2016. 南海北部天然气水合物赋存区沉积物中自生矿物特征及其硫酸盐:甲烷转换带指示意义[D]. 武汉:中国地质大学: 16-79. [Lin Qi. 2016. Authigenic minerals in the sediments from gas hydrate-bearing regions in the northern South China Sea and its implication for sulfate-methane transition zone[D]. Wuhan: China University of Geosciences: 16-79.]
- 王钦贤. 2014. 台湾国姓与甲仙地区冷泉碳酸盐岩石学及地球化学[原文如此][D]. 广州:中国科学院广州地球化学研究所: 13-102. [Wang Qinxian. 2014. Sedimentary and geochemistry of cold seep carbonates from Kuohsing and Chiasien area, Taiwan[sic][D]. Guangzhou: Guangzhou Institute of Geochemistry, Chinese Academy of Sciences: 13-102.]
- 王士伟. 2006. 台湾西南部珊瑚礁在矽质碎屑古环境中最初发育机制之探讨[D]. 台北:台湾大学: 18-149. [Wang Shiwei. 2006. The initial development of coral reefs in siliciclastic paleoenvironments, southwestern Taiwan[D]. Taipei, China: Taiwan University: 18-149.]
- 张文进,王钦贤,陈多福. 2018. 西藏岗巴地区晚白垩世冷泉碳酸盐岩地球化学特征及其对流体来源及沉积环境的示踪[J]. 地球化学, 47(2): 217-227. [Zhang Wenjin, Wang Qinxian, Chen Duofu. 2018. Implications of fluid source and sedimentary environment from the sedimentary geochemistry of Late Cretaceous cold seep carbonates from Gamba, Tibet[J]. *Geochimica*, 47(2): 217-227.]
- 赵若思,王钦贤,陈多福. 2021. 台湾甲仙地区早上新世冷泉白云岩的地质地球化学特征及沉积环境[J]. 海洋地质与第四纪地质, 41(3): 85-94. [Zhao Ruosi, Wang Qinxian, Chen Duofu. 2021. Geochemical characteristics of the Early Pliocene cold seep dolomite at Chiahhsien, Taiwan and their implications for fluid sources and sedimentary environment[J]. *Marine Geology & Quaternary Geology*, 41(3): 85-94.]
- 赵彦彦,李三忠,李达,等. 2019. 碳酸盐(岩)的稀土元素特征及其古环境指示意义[J]. 大地构造与成矿学, 43(1): 141-167. [Zhao Yanyan, Li Sanzhong, Li Da, et al. 2019. Rare earth element geochemistry of carbonate and its paleoenvironmental implications[J]. *Geotectonica et Metallogenia*, 43(1): 141-167.]
- Amano K, Kiel S, Hryniewicz K, et al. 2022. Bivalvia in ancient hydrocarbon seeps[M]//Kaim A, Cochran J K, Landman N H. Ancient hydrocarbon seeps. Cham: Springer: 267-321.
- Arthur M A, Anderson T F, Kaplan I R, et al. 1983. Stable isotopes in sedimentary geology[M]. Tulsa: SEPM Society for Sedimentary Geology: 1-435.
- Bahr A, Pape T, Abegg F, et al. 2010. Authigenic carbonates from the eastern Black Sea as an archive for shallow gas hydrate dynamics—Results from the combination of CT imaging with mineralogical and stable isotope analyses[J]. *Marine and Petroleum Geology*, 27(9): 1819-1829.
- Bian Y Y, Feng D, Roberts H H, et al. 2013. Tracing the evolution of seep fluids from authigenic carbonates: Green Canyon, northern gulf of Mexico[J]. *Marine and Petroleum Geology*, 44: 71-81.
- Birgel D, Feng D, Roberts H H, et al. 2011. Changing redox conditions at cold seeps as revealed by authigenic carbonates from Alaminos Canyon, northern Gulf of Mexico[J]. *Chemical Geology*, 285(1/2/3/4): 82-96.
- Birgel D, Peckmann J, Klautzsch S, et al. 2006. Anaerobic and aerobic oxidation of methane at Late Cretaceous seeps in the western interior seaway, USA[J]. *Geomicrobiology Journal*, 23(7): 565-577.
- Blouet J P, Wetzel A, Ho S. 2021. Fluid conduits formed along burrows of giant bivalves at a cold seep site, southern Taiwan[J]. *Marine and Petroleum Geology*, 131: 105123.
- Boetius A, Ravensschlag K, Schubert C J, et al. 2000. A marine microbial consortium apparently mediating anaerobic oxidation of methane[J]. *Nature*, 407(6804): 623-626.
- Bristow T F, Grotzinger J P. 2013. Sulfate availability and the geological record of cold-seep deposits[J]. *Geology*, 41(7): 811-814.
- Campbell K A. 2006. Hydrocarbon seep and hydrothermal vent paleoenvironments and paleontology: Past developments and future research directions[J]. *Palaeogeography, Palaeoclimatology, Palaeoecology*, 232(2/4): 362-407.
- Campbell K A, Farmer J D, des Marais D. 2002. Ancient hydrocarbon seeps from the Mesozoic convergent margin of California: Carbonate geochemistry, fluids and paleoenvironments[J]. *Geofluids*, 2(2): 63-94.
- Campbell K A, Francis D A, Collins M, et al. 2008. Hydrocarbon seep-carbonates of a Miocene forearc (East Coast Basin), North Island, New Zealand[J]. *Sedimentary Geology*, 204(3/4): 83-105.
- Chen N C, Yang T F, Hong W L, et al. 2017. Production, consumption, and migration of methane in accretionary prism of southwestern Taiwan[J]. *Geochemistry, Geophysics, Geosystems*, 18(8): 2970-2989.
- Chien C W, Huang C Y, Chen Z, et al. 2012. Miocene shallow-marine cold seep carbonate in fold-and-thrust western Foothills, SW Taiwan[J]. *Journal of Asian Earth Sciences*, 56: 200-211.
- Chien C W, Huang C Y, Lee H C, et al. 2013. Patterns and sizes of authigenic carbonate formation in the Pliocene foreland in southwestern Taiwan: Implications of an ancient methane seep[J]. *Terrestrial, Atmospheric and Oceanic Sciences*, 24(6): 971.
- Crusius J, Thomson J. 2000. Comparative behavior of authigenic Re, U, and Mo during reoxidation and subsequent long-term burial in marine sediments[J]. *Geochimica et Cosmochimica Acta*, 64(13): 2233-2242.
- Dubilier N, Bergin C, Lott C. 2008. Symbiotic diversity in marine animals: The art of harnessing chemosynthesis[J]. *Nature Reviews*

- Microbiology, 6(10): 725-740.
- Feng D, Chen D F. 2015. Authigenic carbonates from an active cold seep of the northern South China Sea: New insights into fluid sources and past seepage activity[J]. Deep Sea Research Part II: Topical Studies in Oceanography, 122: 74-83.
- Feng D, Qiu J W, Hu Y, et al. 2018. Cold seep systems in the South China Sea: An overview[J]. Journal of Asian Earth Sciences, 168: 3-16.
- Freslon N, Bayon G, Toucanne S, et al. 2014. Rare earth elements and neodymium isotopes in sedimentary organic matter[J]. Geochimica et Cosmochimica Acta, 140: 177-198.
- Ge L, Qu P F, Zhu B, et al. 2023. Formation process of Pliocene cold seep carbonates from the southern western Foothills, southwestern Taiwan: A synthetic rare earth element and C–O–Sr–Nd isotope study[J]. Marine and Petroleum Geology, 154: 106327.
- Gill F L, Harding I C, Little C T S, et al. 2005. Palaeogene and Neogene cold seep communities in Barbados, Trinidad and Venezuela: An overview[J]. Palaeogeography, Palaeoclimatology, Palaeoecology, 227(1/2/3): 191-209.
- Guan H X, Xu L F, Wang Q X, et al. 2019. Lipid biomarkers and their stable carbon isotopes in ancient seep carbonates from SW Taiwan, China[J]. Acta Geologica Sinica (English Edition), 93(1): 167-174.
- Hammer Ø, Nakrem H A, Little C T S, et al. 2011. Hydrocarbon seeps from close to the Jurassic – Cretaceous boundary, Svalbard[J]. Palaeogeography, Palaeoclimatology, Palaeoecology, 306(1/2): 15-26.
- Hu Y, Feng D, Peckmann J, et al. 2014. New insights into cerium anomalies and mechanisms of trace metal enrichment in authigenic carbonate from hydrocarbon seeps[J]. Chemical Geology, 381: 55-66.
- Huang C Y, Chi W R, Yan Y, et al. 2013. The first record of Eocene tuff in a Paleogene rift basin near Nantou, western Foothills, central Taiwan[J]. Journal of Asian Earth Sciences, 69: 3-16.
- Huang C Y, Chien C W, Zhao M X, et al. 2006. Geological study of active cold seeps in the syn-collision accretionary prism Kaoping slope off SW Taiwan[J]. Terrestrial, Atmospheric and Oceanic Sciences, 17(4): 679-702.
- Huang C Y, Xia K Y, Yuan P B, et al. 2001. Structural evolution from Paleogene extension to Latest Miocene-recent arc-continent collision offshore Taiwan: Comparison with on land geology[J]. Journal of Asian Earth Sciences, 19(5): 619-638.
- Huang C Y, Yen Y, Zhao Q H, et al. 2012. Cenozoic stratigraphy of Taiwan: Window into rifting, stratigraphy and paleoceanography of South China Sea[J]. Chinese Science Bulletin, 57(24): 3130-3149.
- Huang C Y, Yuan P B, Lin C W, et al. 2000. Geodynamic processes of Taiwan arc – continent collision and comparison with analogs in Timor, Papua New Guinea, Urals and Corsica[J]. Tectonophysics, 325(1/2): 1-21.
- Hutchings A M, Basu A, Dickson A J, et al. 2020. Molybdenum geochemistry in salt marsh pond sediments[J]. Geochimica et Cosmochimica Acta, 284: 75-91.
- Iadanza A, Sampalmieri G, Cipollari P, et al. 2013. The “Brecciated Limestones” of Maiella, Italy: Rheological implications of hydrocarbon-charged fluid migration in the Messinian Mediterranean Basin[J]. Palaeogeography, Palaeoclimatology, Palaeoecology, 390: 130-147.
- Jakubowicz M, Dopieralska J, Belka Z. 2015. Tracing the composition and origin of fluids at an ancient hydrocarbon seep (Hollard Mound, Middle Devonian, Morocco): A Nd, REE and stable isotope study[J]. Geochimica et Cosmochimica Acta, 156: 50-74.
- Jiang G Q, Kennedy M J, Christie-Blick N. 2003. Stable isotopic evidence for methane seeps in Neoproterozoic postglacial cap carbonates[J]. Nature, 426(6968): 822-826.
- Joseph C, Campbell K A, Torres M E, et al. 2013. Methane-derived authigenic carbonates from modern and paleoseeps on the Cascadia margin: Mechanisms of formation and diagenetic signals[J]. Palaeogeography, Palaeoclimatology, Palaeoecology, 390: 52-67.
- Kelly S R A, Ditchfield P W, Doubleday P A, et al. 1995. An Upper Jurassic methane-seep limestone from the fossil Bluff Group forearc basin of Alexander Island, Antarctica[J]. Journal of Sedimentary Research, 65(2a): 274-282.
- Kiel S, Aguilar Y, Kase T. 2020. Mollusks from Pliocene and Pleistocene seep deposits in Leyte, Philippines[J]. Acta Palaeontologica Polonica, 65(3): 589-627.
- Kiel S, Birgel D, Peckmann J, et al. 2024. An overview of Miocene to Pleistocene methane-seep faunas from Taiwan: Paleoecology and paleobiogeographic implications[J]. Journal of Asian Earth Sciences, 266: 106119.
- Kiel S, Hansen B T. 2015. Cenozoic methane-seep faunas of the Caribbean region[J]. PLoS One, 10(10): e0140788.
- Liang Q Y, Hu Y, Feng D, et al. 2017. Authigenic carbonates from newly discovered active cold seeps on the northwestern slope of the South China Sea: Constraints on fluid sources, formation environments, and seepage dynamics[J]. Deep Sea Research Part I: Oceanographic Research Papers, 124: 31-41.
- Lu Y, Paulmann C, Mihailova B, et al. 2023. Fibrous dolomite formation at a Miocene methane seep may reflect Neoproterozoic aragonite-dolomite sea conditions[J]. Communications Earth & Environment, 4(1): 346.
- Mellado C, Zambrano N, Aliaga J A, et al. 2022. On the presence of the deep-water mytilid *Gigantidas horikoshii* (Bivalvia: Mytilidae) in Taiwanese waters[sic][J]. Journal of the Marine Biological Association of the United Kingdom, 102(7): 531-534.
- Miao X M, Feng X L, Li J R, et al. 2021. Tracing the paleo-methane seepage activity over the past 20, 000 years in the sediments of Qiongdongnan Basin, northwestern South China Sea[J]. Chemical Geology, 559: 119956.
- Naehr T H, Eichhubl P, Orphan V J, et al. 2007. Authigenic carbonate formation at hydrocarbon seeps in continental margin sediments: A comparative study[J]. Deep Sea Research Part II: Topical Studies

- in *Oceanography*, 54(11/12/13): 1268-1291.
- Nyman S L, Nelson C S. 2011. The place of tubular concretions in hydrocarbon cold seep systems: Late Miocene Urenui Formation, Taranaki Basin, New Zealand[J]. *AAPG Bulletin*, 95(9): 1495-1524.
- Peckmann J, Goedert J L, Thiel V, et al. 2002. A comprehensive approach to the study of methane-seep deposits from the Lincoln Creek Formation, western Washington State, USA[J]. *Sedimentology*, 49(4): 855-873.
- Peckmann J, Reimer A, Luth U, et al. 2001. Methane-derived carbonates and authigenic pyrite from the northwestern Black Sea[J]. *Marine geology*, 177(1/2): 129-150.
- Perri E, Borrelli M, Heimhofer U, et al. 2024. Microbial dominated Ca-carbonates in a giant Pliocene cold-seep system (Croton Basin – South Italy)[J]. *Sedimentology*, 71(6): 1767-1794.
- Pierre C, Blanc-Valleron M M, Caqueneau S, et al. 2016. Mineralogical, geochemical and isotopic characterization of authigenic carbonates from the methane-bearing sediments of the Bering Sea continental margin (IODP Expedition 323, Sites U1343 – U1345) [J]. *Deep Sea Research Part II: Topical Studies in Oceanography*, 125/126: 133-144.
- Reitner J, Blumenberg M, Walliser E O, et al. 2015. Methane-derived carbonate conduits from the Late Aptian of Salinac (Marne Bleues, Vocontian Basin, France): Petrology and biosignatures[J]. *Marine and Petroleum Geology*, 66: 641-652.
- Rickard D. 2019. Sedimentary pyrite framboid size-frequency distributions: A meta-analysis[J]. *Palaeogeography, Palaeoclimatology, Palaeoecology*, 522: 62-75.
- Scholz F, McManus J, Sommer S. 2013. The manganese and iron shuttle in a modern euxinic basin and implications for molybdenum cycling at euxinic ocean margins[J]. *Chemical Geology*, 355: 56-68.
- Scott C, Lyons T W. 2012. Contrasting molybdenum cycling and isotopic properties in euxinic versus non-euxinic sediments and sedimentary rocks: Refining the paleoproxies[J]. *Chemical Geology*, 324/325: 19-27.
- Shields G, Stille P. 2001. Diagenetic constraints on the use of cerium anomalies as palaeoseawater redox proxies: An isotopic and REE study of Cambrian phosphorites[J]. *Chemical Geology*, 175(1/2): 29-48.
- Smrzka D, Zwicker J, Kolonic S, et al. 2017. Methane seepage in a Cretaceous greenhouse world recorded by an unusual carbonate deposit from the Tarfaya Basin, Morocco[J]. *The Depositional Record*, 3(1): 4-37.
- Stakes D S, Orange D, Paduan J B, et al. 1999. Cold-seeps and authigenic carbonate formation in Monterey Bay, California[J]. *Marine Geology*, 159(1/2/3/4): 93-109.
- Stanley S M. 1970. Relation of shell form to life habits of the Bivalvia (Mollusca)[M]. *America: Geological Society of America*: 1-282.
- Takeuchi R, Matsumoto R, Ogihara S, et al. 2007. Methane-induced dolomite “chimneys” on the Kuroshima Knoll, Ryukyu islands, Japan[J]. *Journal of Geochemical Exploration*, 95(1/2/3): 16-28.
- Taylor J D, Glover E A. 2000. Functional anatomy, chemosymbiosis and evolution of the Lucinidae[J]. *Geological Society, London, Special Publications*, 177(1): 207-225.
- Tong H P, Feng D, Cheng H, et al. 2013. Authigenic carbonates from seeps on the northern continental slope of the South China Sea: New insights into fluid sources and geochronology[J]. *Marine and Petroleum Geology*, 43: 260-271.
- Tong H P, Feng D, Peckmann J, et al. 2019. Environments favoring dolomite formation at cold seeps: A case study from the gulf of Mexico[J]. *Chemical Geology*, 518: 9-18.
- Tribouillard N, du Châtelet E A, Gay A, et al. 2013. Geochemistry of cold seepage-impacted sediments: Per-ascensum or per-descensum trace metal enrichment?[J]. *Chemical Geology*, 340: 1-12.
- Utsunomiya M, Majima R, Taguchi K, et al. 2015. An *in situ* vesicomid-dominated cold-seep assemblage from the lowermost Pleistocene Urago Formation, Kazusa Group, forearc basin fill on the northern Miura Peninsula, Pacific side of central Japan[J]. *Paleontological Research*, 19(1): 1-20.
- Viola I, Oppo D, Franchi F, et al. 2015. Mineralogy, geochemistry and petrography of methane-derived authigenic carbonates from Enza River, northern Apennines (Italy)[J]. *Marine and Petroleum Geology*, 66: 566-581.
- Wang Q X, Tong H P, Huang C Y, et al. 2018. Tracing fluid sources and formation conditions of Miocene hydrocarbon-seep carbonates in the central western Foothills, central Taiwan[J]. *Journal of Asian Earth Sciences*, 168: 186-196.
- Wang S W, Gong S Y, Mii H S, et al. 2006. Cold-seep carbonate hardgrounds as the initial substrata of coral reef development in a siliciclastic paleoenvironment of southwestern Taiwan[J]. *Terrestrial, Atmospheric and Oceanic Sciences*, 17(2): 405-427.
- Wang X, Barrat J A, Bayon G, et al. 2020. Lanthanum anomalies as fingerprints of methanotrophy[J]. *Geochemical Perspectives Letters*, 14: 26-30.
- Wang X D, Guan H X, Qiu J W, et al. 2022. Macro-ecology of cold seeps in the South China Sea[J]. *Geosystems and Geoenvironment*, 1(3): 100081.
- Wilkin R T, Barnes H L, Brantley S L. 1996. The size distribution of framboidal pyrite in modern sediments: An indicator of redox conditions[J]. *Geochimica et Cosmochimica Acta*, 60(20): 3897-3912.
- Ye Y, Zhang S, Wang H, et al. 2021. Black shale Mo isotope record reveals dynamic ocean redox during the Mesoproterozoic Era[J]. *Geochemical Perspectives Letters*, 18: 16-21.
- Zhang X L, Chen K F, Hu D P, et al. 2016. Mid-Cretaceous carbon cycle perturbations and Oceanic Anoxic Events recorded in southern Tibet[J]. *Scientific Reports*, 6(1): 39643.
- Zwicker J, Smrzka D, Himmler T, et al. 2018. Rare earth elements as tracers for microbial activity and early diagenesis: A new perspective from carbonate cements of ancient methane-seep deposits[J]. *Chemical Geology*, 501: 77-85.

## Geological and Geochemical Characteristics of Ancient Cold Seep Carbonates in Taiwan Area, China

ZANG YiPing, WANG QinXian, JIA ZiCe, CHEN DuoFu

College of Oceanography and Ecological Science, Shanghai Ocean University, Shanghai 201306, China

**Abstract:** [Significance] Cold seep activity has a significant impact on marine ecosystems and global climate change, and has been widely developed globally at active and passive continental margins. The fundamental process operating at seeps is the anaerobic oxidation of methane (AOM) mediated by a combination of anaerobic methanotrophic archaea (ANME) and sulfate-reducing bacteria (SRB). This increases the alkalinity of pore water, forming a favorable environment for carbonate mineral precipitation. Cold seep carbonates are the product of submarine cold seep activity, and their geological and geochemical characteristics are often used to trace seepage fluid information and changes in sedimentary environments. [Progress] Taiwan area of China is located in the collision zone between the Luzon Island Arc of the Philippine Sea Plate and the Eurasian continental margin, and possesses complex geological structures such as extensive faults, providing appropriate conditions for the development of cold seeps. Cold seep carbonates in the Taiwan area are mainly found in Miocene to Pleistocene strata, which are ideal for the study of ancient cold seeps. A relatively detailed study has been conducted on their fundamental geological and geochemical properties, including mineralogy, petrology and carbon and oxygen isotope content. This study includes a comprehensive analysis of the geological occurrence, mineralogical and petrological characteristics, carbon and oxygen isotopes content, rare earth element (REE) geochemistry, and macrofossil content of cold seep carbonates in the Taiwan area. In addition, it explores the fluid seepage activities and the depositional environment recorded by the cold seep carbonates, taking account of the geological and geochemical features of cold seep carbonates from other regions globally. [Conclusions and Prospects] The predominantly blocky and chimney-like forms of the cold seep carbonates in the Taiwan area indicate two types of seepage activity: the blocky forms indicate prolonged periods of low-flux diffuse seepage; the chimney-like forms represent shorter periods of high-flux convective seepage. The primary carbonate minerals are dolomite and calcite, with a significant presence of framboidal pyrites. The size of the pyrite grains may be related to the redox conditions during deposition. The carbon isotope composition of cold seep carbonates indicates that the primary sources of carbon were biogenic and thermogenic methane, with additional influence of seawater or residual CO<sub>2</sub> from methanogenesis. Notably, Pliocene cold seep carbonates exhibit the widest range in carbon isotope values, suggesting a greater diversity of carbon sources, potentially due to the complex geological structures in Taiwan area at that time. Furthermore, the  $\delta^{18}\text{O}$  values of cold seep carbonates from the Miocene to the Pleistocene in the Taiwan area exhibit an increasingly positive trend, suggesting that these carbonates might have undergone a transition from gas hydrate formation to dissociation and release. The geochemical characteristics of the REE indicate a predominantly reducing depositional environment. The cold seep macrofossils are dominated by bivalves, representing few biological species in the Miocene and Pliocene but a greater range in the Pleistocene, possibly as a result of different water depths. For greater in-depth understanding of the ancient cold seep systems in the Taiwan area, future research on cold seep carbonates could focus on *in situ* micro-scale analysis of carbon and oxygen isotopes, and molybdenum element and isotope, in the carbonate minerals, as well as the spatial differences in the growth of macrofauna of different genera of the *Lucinidae* family, in conjunction with geochemical analysis.

**Key words:** carbonate; ancient cold seep; Taiwan area of China; carbon source; sedimentary environment; macrofauna

---

**Foundation:** National Natural Science Foundation of China, No. 42172110

**Corresponding author:** WANG QinXian, E-mail: qxwang@shou.edu.cn